Polyhedron 47 (2012) 134–142

Contents lists available at SciVerse ScienceDirect

Polyhedron

journal homepage: www.elsevier.com/locate/poly

The influence of substituents (R) at N^1 atom of furan-2-carbaldehyde thiosemicarbazones $\{(C_4H_3O)HC^2{=}N^3{-}N(H){-}C^1(=S)N^1HR\}$ on bonding, nuclearity, H-bonded networks of copper(I) complexes

Tarlok S. Lobana [a,*], Rekha Sharma [a], Geeta Hundal [a], A. Castineiras [b], Ray Jay Butcher [c]

[a] Department of Chemistry, Guru Nanak Dev University, Amritsar 143005, India
[b] Departamento De Quimica Inorganica, Facultad de Farmacia, Universidad de Santiago, 15782 Santiago, Spain
[c] Department of Chemistry, Howard University, Washington, DC 20059, USA

ARTICLE INFO

Article history:
Received 23 January 2012
Accepted 6 August 2012
Available online 16 August 2012

Keywords:
Furane-2-carbaldehyde-N^1-methyl thiosemicarbazone
Three-coordinated monomers
S-bridged dimer
Copper(I) halides
Triphenylphosphine
Iodide-bridged dimer

ABSTRACT

The chemistry of copper(I) halides (CuX) with furan-2-carbaldehyde-N^1-substituted thiosemicarbazones $\{(C_4H_3O)HC^2{=}N^3N^2H{-}C^1(=S)N^1HR$, Hftsc-$N^1HR\}$ in presence of triphenyl phopshine is described. For methyl and ethyl substituents (R) at N^1 atom, and with X = I, Br, Cl, the halogen-bridged dimers, namely, $[Cu_2(\mu\text{-}X)_2(\eta^1\text{-}S\text{-}Hftsc\text{-}N^1HR)_2(PPh_3)_2]$ (R, X: Me, I, **1**, Br **2**, Cl **3**; Et, I **4**, Br **5**, Cl **6**) have been obtained.

However, the presence of phenyl substituent at N^1 has favored a three coordinate complex, $[CuI(\eta^1\text{-}S\text{-}Hftsc\text{-}N^1HPh)_2]$ **7**, and with copper(I) bromide/and chloride, it has formed sulfur-bridged dimers, $[Cu_2X_2(\eta^1\text{-}Hftsc\text{-}N^1HPh)_2(\mu\text{-}S\text{-}Hftsc\ N^1HPh)_2]$ (X = Br **8**, Cl **9**). In the latter three complexes (**7**–**9**), the Ph_3P ligand did not take part in coordination. All these complexes have been characterized with the help of elemental analysis, IR, ^{1}H NMR spectroscopy and X-ray crystallography (**1**–**3**, **5**, **7** and **9**). The bonding and nuclearity of complexes has been found to vary with the substituents at N^1 atom. The intermolecular interactions have formed one dimensional (**1**, **9**) and two dimensional (**2**, **3** and **5**) networks.

1. Introduction

Thiosemicarbazones $\{R^1R^2C^2(=N^3)N^2HC(=S)N^1H_2\}$ are versatile N, S donor ligands with potential to bind to a metal via one or more donor atoms. The importance of thiosemicarbazones lies in their structural diversity [1–8], ion-sensing ability [9–12], metal extraction properties [13,14] and pharmacological properties [15–18]. Thiosemicarbazones containing heterocyclic rings at C^2 carbon like pyrrole or thiophene or pyridine are extensively studied, however, thiosemicarbazones having furan ring is less studied for their interactions with the metals. Only a few complexes, namely, $[Ni(ftsc)_2]$ [19], $[Ni(mftsc)_2]$ (mftsc = anion of 5-methyl-2-furanaldehyde thosemicarbazone) [20], $[CuI(Hftsc)(Ph_3P)]_2$ [21a], $[CuCl(HftscMe)]_2$ [21b], $[Cu(ftsc)_2]$ [22], $[CuCl_2(Hftsc)]$ [23], $[Ag(Hftsc)(Ph_3P)]_2(NO_3)_2$ [7] and $[Ga(ftscMe)Me_2]$ (ftscMe = furan-2-carbaldehyde-N-methyl-thiosemicarbazonate) [24] are structurally characterized. The furan based neutral thiosemicarbazones have shown two types of bonding modes, namely, η^1-S (mode A) [21], μ-S (mode B) and N^3, S-chelation-cum-S-bridging (mode C) [7], however, in anionic form it has shown N^3, S-chelation (mode D) [22] (Chart 1).

Recently, the chemistry of copper(I) halides with thiophene-2-carbaldehyde thiosemicarbazones has been reported [25,26]. The substituents at C^2 and N^1 atoms influenced the bonding and nuclearity of copper(I) halide complexes. Herein we describe the effect of substituents at N^1 atoms of furan-2-carbaldehyde thiosemicarbazones as shown in Chart 2. Triphenyl phosphine has been used as co-ligand as it helps to solubilize the reaction contents and also helps in the formation of crystals. The products have been characterized by IR and ^{1}H NMR spectroscopies, and several of them by X-ray crystallography.

2. Materials and techniques

Copper(I) halides were prepared by the reduction of $CuSO_4{\cdot}5H_2O$ using SO_2 in the presence of NaX (X = Cl, Br, I) in distilled water [27]. The N^1-methyl-thiosemicarbazide, N^1-ethyl-thiosemicarbazide, N^1-phenyl-thiosemicarbazide and Ph_3P were procured from Aldrich Sigma Ltd. Thiosemicarbazone ligands were prepared by condensation of furanaldehyde with respective thiosemicarbazides as previously reported [1,25,26]. The elemental analysis for C, H and N were carried out using a thermoelectron FLASHEA1112 analyzer. The melting points were determined with a Gallenkamp electrically heated apparatus. The I.R spectra of the ligands and the complexes were recorded in the range, 4000–400 cm^{-1} (using KBr pellets) on the FTIR-SHIMADZU 8400 Fourier Transform

* Corresponding author. Tel.: +91 93175 98845; fax: +91 183 2258820.
E-mail address: tarlokslobana@yahoo.co.in (T.S. Lobana).

0277-5387/$ - see front matter © 2012 Elsevier Ltd. All rights reserved.
http://dx.doi.org/10.1016/j.poly.2012.08.014

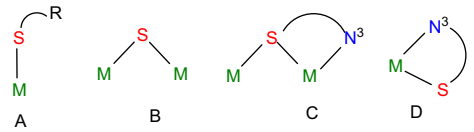

Chart 1. Bonding modes.

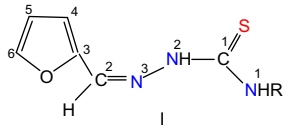

R = H furan-2-carbaldehyde thiosemicarbazone (Hftsc-NH_2)
Me furan-2-carbaldehyde-N^1-methyl thiosemicarbazone (Hftsc-N^1HMe)
Et furan-2-carbaldehyde-N^1-ethyl thiosemicarbazone (Hftsc-N^1HEt)
Ph furan-2-carbaldehyde-N^1-phenyl thiosemicarbazone(Hftsc-N^1HPh)

Chart 2.

Spectrophotometer and on Pye–Unicam SP-3-300 spectrophotometer. The ^{1}H NMR spectra were recorded on a JEOL AL300 FT spectrometer at 300 MHz in $CDCl_3$ with TMS as the internal reference.

2.1. Synthesis of complexes

2.1.1. Synthesis of $[Cu_2(\mu\text{-}I)_2(\eta^1\text{-}S\text{-}Hftsc\text{-}N^1HMe)_2(Ph_3P)_2]$ (**1**)

To copper(I) iodide (0.025 g, 0.131 mmol) dissolved in acetonitrile (15 mL), the HftscMe ligand (0.024 g, 0.131 mmol) was added and the contents were stirred for 3–4 h. It formed yellow precipitate and to the precipitate, the co-ligand Ph_3P (0.034 g, 0.131 mmol) was added and after stirring for 5–10 min, it formed a yellow solution. Slow evaporation of the solution at room temperature gave yellow crystals. Yield, 74%, m.p. 205–207 °C. *Anal.* Calc. for $C_{50}H_{48}Cu_2I_2N_6S_2O_2P_2$: C, 41.21; H, 3.78; N, 6.61. Found: C, 41.19; H, 3.52; N, 6.19%.). IR data (KBr, cm^{-1}): ν(N–H), 3310m, 3143m, 3129m; (–NHMe + N^2H), ν(C–H), 3010m, 2983m, 2822m; ν(C=N) + ν(C–C), 1550s, 1520s; ν(C–N), 1066s, 1039s, 936s; ν(C=S), 865s; ν(P–C_{Ph}), 1094(s). ^{1}H NMR ($CDCl_3$, δ ppm): 12.23 (s, 1H, N^2H), 8.19 (s, 1H, C^2H), 7.36–7.67 (m, 18H, C^6H, 3Ph, N^1H), 6.75 (d,1H, C^4H), 6.51 (dd, 1H, C^5H), 3.21 (d, 2H, CH_3).

Complexes **2**–**6** were prepared by the same method.

2.1.2. Synthesis of $[Cu_2(\mu\text{-}Br)_2(\eta^1\text{-}S\text{-}Hftsc\text{-}N^1HMe)_2(Ph_3P)_2]$ (**2**)

Yield, 65%, m.p. 210–212 °C. *Anal.* Calc. for $C_{50}H_{48}Cu_2Br_2N_6S_2O_2P_2$: C, 50.98; H, 4.08; N, 7.14. Found: C, 50.38; H, 3.99; N, 7.41%. IR data (KBr, cm^{-1}): ν(N–H), 3315m, 3146m, 3120m (–NHMe + N^2H); ν(C–H), 3016m, 2990m, 2843m; ν(C=N) + ν(C–C), 1560s, 1529s; ν(C–N), 1060s, 1029s, 935s; ν(C=S), 863s; ν(P–C_{Ph}), 1092(s). ^{1}H NMR ($CDCl_3$, δ ppm): 11.58 (s, 1H, N^2H), 8.22 (s, 1H, C^2H), 7.37–7.65 (m, 18H, C^6H, 3Ph, N^1H), 6.72 (d,1H, C^4H), 6.51 (dd, 1H, C^5H), 3.19 (d, 2H, CH_3).

2.1.3. Synthesis of $[Cu_2(\mu\text{-}Cl)_2(\eta^1\text{-}S\text{-}Hftsc\text{-}N^1HMe)_2(Ph_3P)_2]$ (**3**)

Yield, 69%, m.p. 202–205 °C. *Anal.* Calc. for $C_{50}H_{48}Cu_2Cl_2N_6S_2O_2P_2$: C, 55.14; H, 4.41; N, 7.72. Found: C, 55.26; H, 4.48; N, 7.62%. IR data (KBr, cm^{-1}): ν(N–H), 3316m, 3148m, 3122m (–NHMe + N^2H); ν(C–H), 3016m, 2976m, 2832m; ν(C=N) + ν(C–C), 1555s, 1529s; ν(C–N), 1056s, 1029s, 938s; ν(C=S), 862s; ν(P–C_{Ph}), 1092(s). ^{1}H NMR ($CDCl_3$, δ ppm): 12.56 (s, 1H, N^2H), 8.17 (s, 1H, C^2H), (C^2H), 7.37–7.68 (m, 18H, C^6H, 3Ph, N^1H), 6.75 (d,1H, C^4H), 6.50 (dd, 1H, C^5H), 3.20 (d, 2H, CH_3).

2.1.4. Synthesis of $[Cu_2(\mu\text{-}I)_2(\eta^1\text{-}S\text{-}Hftsc\text{-}N^1HEt)_2(Ph_3P)_2]$ (**4**)

Yield, 73%, m.p. 205–207 °C. *Anal.* Calc. for $C_{52}H_{52}Cu_2I_2N_6S_2O_2P_2$: C, 48.04; H, 4.60; N, 6.47. Found: C, 48.24; H, 4.33; N, 6.27%. IR data (KBr, cm^{-1}): ν(N–H), 3264m, 3252m, (–NHEt + N^2H); ν(C–H), 3087m, 3010m, 2879m; ν(C=N) + ν(C–C), 1565s, 1530s; ν(C–N), 1075s, 1033s, 925s; ν(C=S), 867s; ν(P–C_{Ph}), 1093(s). ^{1}H NMR ($CDCl_3$, δ ppm): 12.24s (s, 1H, N^2H), 8.17 (s, 1H, C^2H), 7.31–7.69 (m, 18H, C^6H, 3Ph, N^1H), 6.76 (d,1H, C^4H), 6.50 (dd, 1H, C^5H), 3.63 (m, 2H, CH_2), 1.33 (t, 3H, CH_3).

2.1.5. Synthesis of $[Cu_2(\mu\text{-}Br)_2(\eta^1\text{-}S\text{-}Hftsc\text{-}N^1HEt)_2(Ph_3P)_2]$ (**5**)

Yield, 71%, m.p. 198–200 °C. *Anal.* Calc. for $C_{52}H_{52}Cu_2Br_2N_6S_2O_2P_2$: C, 51.78; H, 4.31; N, 6.97. Found: C, 51.66; H, 4.24; N, 6.83%. IR data (KBr, cm^{-1}): ν(N–H), 3260 m, 3242 m, (–NHEt + N^2H); ν(C–H), 3095m, 3014m, 2877m; ν(C=N) + ν(C–C), 1570s, 1539s; ν(C–N), 1056s, 1030s, 931s; ν(C=S), 866s; ν(P–C_{Ph}), 1094(s). ^{1}H NMR ($CDCl_3$, δ ppm): 12.51 (s, 1H, N^2H), 8.19 (s, 1H, C^2H), 7.31–7.65 (m, 18H, C^6H, 3Ph, N^1H), 6.74 (d,1H, C^4H), 6.51 (dd, 1H, C^5H), 3.69 (m, 2H, CH_2), 1.31 (t, 3H, CH_3).

2.1.6. Synthesis of $[Cu_2(\mu\text{-}Cl)_2(\eta^1\text{-}S\text{-}Hftsc\text{-}N^1HEt)_2(Ph_3P)_2]$ (**6**)

Yield, 69%, m.p. 180–182 °C. *Anal.* Calc. for $C_{52}H_{52}Cu_2Cl_2N_6S_2O_2P_2$: C, 55.91; H, 4.65; N, 7.52. Found: C, 55.69; H, 4.69; N, 7.63%. IR data (KBr, cm^{-1}): ν(N–H), 3265m, 3245m, (–NHEt + N^2H); ν(C–H), 3098m, 3017m, 2876m; ν(C=N) + ν(C–C), 1575s, 1539s; ν(C–N), 1056s, 1033s, 935s; ν(C=S), 862s; ν(P–C_{Ph}), 1092(s). ^{1}H NMR ($CDCl_3$, δ ppm): 12.50 (s, 1H, N^2H), 8.18 (s, 1H, C^2H), 7.31–7.63 (m, 18H, C^6H, 3Ph, N^1H), 6.74 (d,1H, C^4H), 6.49 (dd, 1H, C^5H), 3.67 (m, 2H, CH_2), 1.32 (t, 3H, CH_3).

2.1.7. Synthesis of $[CuI(\eta^1\text{-}S\text{-}Hftsc\text{-}N^1HPh)_2]$ (**7**)

To copper(I) iodide (0.025 g, 0.131 mmol) in acetonitrile (15 mL), the ligand HftscPh (0.034 g, 0.131 mmol) was added, and the contents were stirred for 3–4 h. It formed yellow precipitates and addition of Ph_3P (0.034 g, 0.131 mmol) followed by stirring for 5–10 min formed a yellow solution, which on slow evaporation at room temperature yielded brown crystals. Yield, 34%, m.p. 170–172 °C. *Anal.* Calc. for $C_{24}H_{22}O_2S_2CuI$: C, 42.32; H, 3.23; N, 12.34. Found: C, 42.24; H, 3.26; N, 12.34%. IR data (KBr, cm^{-1}): ν(N–H), 3290s, 3122m, 3107m, (–NHPh + N^2H); ν(C–H), 2987m, 2979m; ν(C=N) + ν(C–C), 1550s, 1530s; ν(C–N), 1076s, 1014s, 928s; ν(C=S), 867m. ^{1}H NMR ($CDCl_3$, δ ppm): 12.24 (s, 1H, N^2H), 8.98 (s, 1H, C^2H), 8.29 (s, 1H, C^6H), 7.28–7.56 (m, 6H, Ph, N^1H), 6.83 (d, 1H, C^4H), 6.53 (dd, 1H, C^5H),. Complexes **8** and **9** were prepared similarly.

2.1.8. Synthesis of $[Cu_2Br_2(\mu\text{-}S\text{-}Hftsc\text{-}N^1HPh)_2(\eta^1\text{-}S\text{-}Hftsc\text{-}N^1HPh)_2]\cdot 2CH_3CN$ (**8**)

Brown crystals. Yield, 42%, m.p. 205–207 °C. *Anal.* Calc. for $C_{52}H50Cu_2Br_2N_{14}O_4S_4$: C, 39.12; H, 3.13; N, 12.28. Found: C, 39.20; H, 3.12; N, 12.29%. IR data (KBr, cm^{-1}): ν(N–H), 3292s, 3115m, 3100m, (–NHPh + N^2H); ν(C–H), 2983m, 2972m; ν(C=N) + ν(C–C), 1560s, 1529s; ν(C–N), 1067s, 1012s, 928s; ν(C=S), 865m. ^{1}H NMR ($CDCl_3$, δ ppm): 12.43 (s, 1H, N^2H), 8.78 (s, 1H, C^2H), 7.69 (s, 1H, C^6H), 7.24–7.59 (m, 6H, Ph, N^1H), 6.75 (d, 1H, C^4H), 6.54 (dd, 1H, C^5H).

2.1.9. Synthesis of $[Cu_2Cl_2(\mu\text{-}S\text{-}Hftsc\text{-}N^1HPh)_2(\eta^1\text{-}S\text{-}Hftsc\text{-}N^1HPh)_2]\cdot 2CH_3CN$ (**9**)

Brown crystals. Yield, 35%, m.p. 203–205 °C. *Anal.* Calc. for $C_{52}H_{50}Cu_2Cl_2N_{14}S_4O_4$: C, 49.52; H, 3.97; N, 15.55. Found: C, 49.49; H, 3.87; N, 15.54%. IR data (KBr, cm^{-1}): ν(N–H), 3293s, 3122m, 3117m, (–NHPh + N^2H); ν(C–H), 2987m, 2986m; ν(C=N) + ν(C–C), 1555s, 1530s; ν(C–N), 1076s, 1020s, 928s; ν(C=S), 863m. ^{1}H NMR ($CDCl_3$, δ ppm): 12.20 (s, 1H, N^2H), 8.84 (s, 1H, C^2H), 7.64

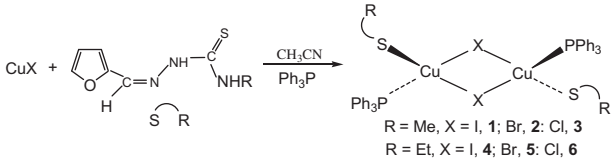

Scheme 1.

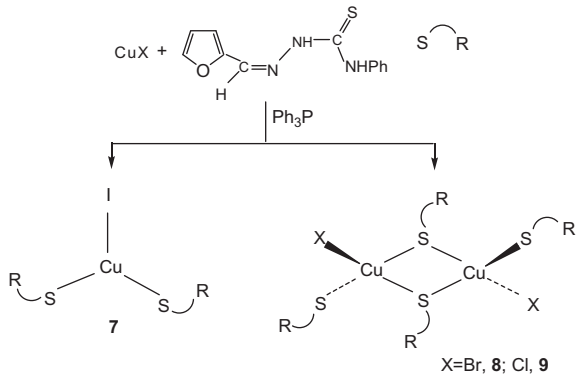

Scheme 2.

(s, 1H, C^6H), 7.26–7.60 (m, 6H, Ph, N^1H), 6.70 (d, 1H, C^4H), 6.65 (dd, 1H, C^5H).

2.2. .X-ray data collection, structure solution and refinement

The data were collected on a Siemens P4 diffractometer using XSCANS [28] for **1** and **3**, on a Bruker SMART CCD 1000 for **2**, an automatic Enraf-Nonius CAD-4 diffractometer and Xcalibur for **5**, **9** and Ruby, Gemini for **7**. All these diffracometers are equipped with graphite monochromated MoK_α radiation ($\lambda = 0.71073$ Å). Data were collected and refined on Siemens XSCANS and data reduction was done by SHELXTL-PC [29] for **1** and **3**. The data were processed with SAINT [30], corrected using SADABS for **2** [31] and solved and refined by SHELXL-97, in **2** and **7** [32] for **2** and XCAD-49 and SHELXL-97 [33] for **5** and **9**.

3. Results and discussion

3.1. General comments on synthesis

Scheme 1 shows the formation of complexes. Furan-2-carbaldehyde-N^1-methyl thiosemicarbazone (Hftsc-N^1HMe) with copper(I) iodide in acetonitrile with Ph_3P as co-ligand has yielded an iodide bridged dinuclear complex, $[Cu_2(\mu\text{-}I)_2(\eta^1\text{-S-Hftsc-}N^1\text{HMe})_2(Ph_3P)_2]$ **1**. The thio-ligand, Hftsc-N1H2 (R = H) with copper(I) iodide also yielded a similar dimer, $[Cu_2(\mu\text{-}I)_2(\eta^1\text{-S-Hftsc-}N^1H_2)_2(Ph_3P)_2]$ [21]. Both these dimers are similar to those formed with thiophene-2-carbaldehyde- and thiophene-2-carbaldehyde-N^1-methyl thiosemicarbazones [21,25]. Other copper(I) halides with furan-2-carbaldehyde-N^1-methyl/ethyl-thiosemicarbazones have also yielded halide bridged dimers, $[Cu_2(\mu\text{-}X)_2(\eta^1\text{-S-Hftsc-}N^1\text{HR})_2(Ph_3P)_2]$ (R, X: Me, Br, **2**; Me, Cl, **3**; Et, I, **4**; Et, Br, **5**; Et, Cl, **6**) (Scheme 1). Complexes **2**–**6** are similar to the corresponding thiophene-2-carbaldehyde-N1-methyl (or ethyl) thiosemicarbazones [25]. It is remarked here that theoretically it has been demonstrated that the halogen-bridging is a favored mode of bonding in copper-thiosemicarbazone chemistry unless halogen is engaged in some sort of hydrogen bonding with a solvent or water from the system [21,26].

Another thio-ligand, namely, furan-2-carbaldehyde-N^1-phenyl thiosemicarba-zone (Hftsc-N^1HPh), has shown a different coordination behavior. Two types of products have been isolated, namely, a three coordinate complex, $[CuI(\eta^1\text{-S-HftscPh})_2]$ **7**, and sulfur-bridged dimers, $[Cu_2(\eta^1\text{-X})_2(\mu\text{-S-Hftsc-}N^1\text{HPh})_2(\eta^1\text{-S-Hftsc-}N^1\text{HPh})_2]\cdot 2CH_3CN$ (X = Br, **8**; Cl, **9**) (Scheme 2). The mixing ratios were same as for **1**–**6**, but Ph_3P did not show coordination to Cu^I metal center. It is an unusual behavior and may be attributed to the presence of phenyl substituent at N^1 atom. Thus basically in complexes **7**–**9**, the copper(I) halides are bonded to two thio-ligands and one halogen, CuX(Hftsc-N1HPh)$_2$, which probably dimerise through sulfur for X = Br, Cl (**8**, **9**) and remain three coordinated for X = I (**7**). In comparison, thiophene-2-carbaldehyde-N1-phenyl thiosemicarbazone (Httsc-N1HPh) was found to form with copper(I) iodide three coordinate monomer and its sulfur-bridged dimer in the same unit cell. On the other hand with copper(I)chloride and bromide, it formed three coordinate complexes as shown in Scheme 3 [25]. Thus furan and thiophene based thio-ligands showed different behavior for phenyl substituent at N^1 atom.

The presence of ν(N–H) bands in the ranges 3265–3316 cm^{-1} (due to $-N^1HR$) and 3242–3100 cm^{-1} due to $-N^2H-$ in IR spectra of complexes revealed that neutral ligand is coordinated to the copper center. The thioamide bands due to ν(C=S) undergo low energy shifts at 862–867 cm^{-1} in complexes (free ligands, 880–887 cm^{-1}). In complexes **1**–**6**, the appearance of νP−CPh) bands in the ranges 1092−1095 cm^{-1} indicate coordinated Ph_3P ligand.

3.2. Molecular structures (*1*–*3*, *5*, *7* and *9*)

The crystallographic data, important bond parameters of compounds **1**–**3**, **5**, **7**, **9** and its comparison with literature are given in Tables 1–4. The molecular structures of representative complexes (**1**, **7** and **9**) are given in Figs. 1–3. Complexes **1**–**3**, **5** and **9** crystallized in triclinic system with space group $P\bar{1}$, whereas complex **7** crystallized in monoclinic group with space group $P2_1/c$. These complexes are divided into three categories: (i) halogen-bridged dimers, $[Cu_2(\mu\text{-}X)_2(\eta^1\text{-S-HL})_2(Ph_3P)_2]$ (HL = Hftsc-N^1HMe,

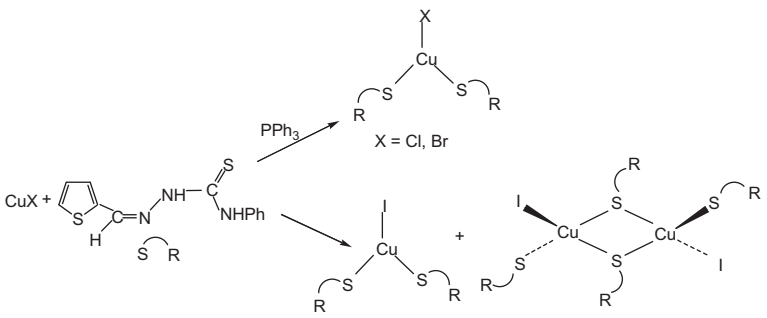

Scheme 3.

Table 1
A comparison of important parameters (bond length, Å; bond angle, °) of dinuclear-copper(I) complexes.

R^1, R^2, R^3[a]	Cu–S	I–Cu–I	Cu–I–Cu	Cu...Cu	Ref.
Comparison of iodo-bridged dimers with different R^1, R^2, R^3					
	2.3017(2)	99.43(2)	80.57(2)	3.5043	[37]
	2.3098(2)	97.28(3)	82.72(3)	3.606(1)	[37]
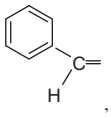	2.3399(9)	111.91(3)	68.087(16)	2.9786	[38]
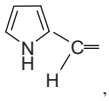	2.331(4)	109.28(7)	70.72(7)	3.097(4)	[39]
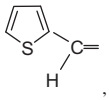	2.3284(8)	106.819(15)	73.571(13)	3.3509	[21]
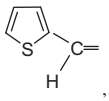	2.3306(4)	107.06(2)	72.934(6)	3.2213	[25]
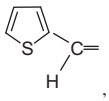	2.3214(14)	103.029(18)	76.971(1)	3.377	[25]
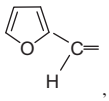	2.340(9)	112.001(16)	67.999(16)	2.9808(8)	[21]
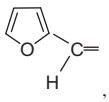	2.3336(13)	108.20(2)	71.80(2)	3.187	[25]
Comparison of sulfur-bridged dimers with different R^1, R^2, R^3					
R^1, R^2, R^3 (X)	Cu–S	S–Cu–S	Cu–S–Cu	Cu...Cu	Ref.
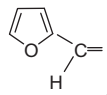	2.2833(3), 2.5955(4)	100.738(12)	69.89(11)	2.8060(3)	[36]
(Cl) 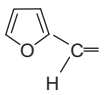	2.2829(5), 2.7583(5)	99.546(15)	80.454(15)	3.276	This paper
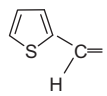	2.2641(9), 2.8006 (10)	104.16(3)	75.84(3)	3.141	[36]
(Cl) 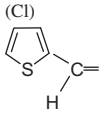	2.2961(9), 2.6553(11)	97.33(3)	82.67(3)	3.281	[25]

[a] R^1R^2=NNHC(=S)NHR^3.

Hftsc N^1HEt) **1**–**3**, **5**, (ii) three coordinated monomer, [CuI(η^1-S-Hftsc-N^1HPh)$_2$] **7** and (iii) sulfur-bridged dimer, [Cu_2Cl_2(μ-S-Hftsc-N^1HPh)$_2$(η^1-S-Hftsc-N^1HPh)$_2$] **9**. Complexes **1**–**3**, **5** are halogen bridged dimers. Here one halogen atom, one thione sulfur and one P donor of PPh_3 appear to have formed a three-coordinate unit which dimerizes via halogen to form halogen bridged dimers [Cu_2(μ-X)$_2$(η^1-S-HL)$_2$(Ph_3P)$_2$] (HL = Hftsc-N^1HMe, X = I **1** (Fig. 1); Br, **2**; Cl, **3**: Hftsc-N^1HEt, Br **5**). The central Cu(μ-X)$_2$Cu core in all these complexes is parallelogram with unequal Cu–X bond distances (Table 4).

It can be observed that if we keep the ligand constant as for example in complexes of Hftsc-N^1HMe, the Cu–S bond distances

Table 2
Important bond parameters of three-coordinated complexes, $[CuX(Htsc)_2]$.

R^1, R^2 (R^3)[a]	X	Cu–S	Cu–X	X–Cu–S	S–Cu–S	Ref.
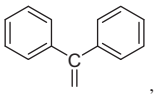	I	2.2269(7) 2.2321(7)	2.5441	119.62(3)	121.42(2)	[35]
(H) 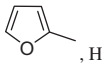 , H	I	2.2367(7) 2.2422(8)	2.5479(4)	123.83(2)	109.88(3)	This paper
(Ph) 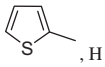 , H	I	2.2526(9) 2.2613(9)	2.5876(5)	123.53(3)	112.63(3)	[25]
(Ph) 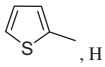 , H	Br	2.2201(8) 2.2387(7)	2.4207(4)	122.45(3)	116.13(3)	[25]
(Ph) 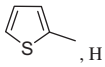 , H	Cl	2.214(3) 2.234(3)	2.295(3)	121.73(9)	116.21(10)	[25]
(Ph) 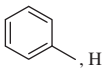 , H (Me)	Cl	2.223(3) 2.226(4)	2.3055(3)	119.96(12)	121.10(6)	[36]

[a] R^1R^2=NNHC(=S)NHR^3.

Table 3
Crystallographic data of complexes.

	1	**2**	**3**
Empirical formula	$C_{50}H_{48}Cu_2I_2N_6O_2P_2S_2$	$C_{50}H_{48}Br_2Cu_2N_6O_2P_2S_2$	$C_{50}H_{48}Cl_2Cu_2N_6O_2P_2S_2$
Crystal system	triclinic	triclinic	triclinic
Space group	$P\bar{1}$	$P\bar{1}$	$P\bar{1}$
a (Å)	10.901(5)	10.4280(8)	10.7050(10)
b (Å)	10.963(5)	10.8034(8)	10.9210(10)
c (Å)	11.797(5)	12.9144(10)	12.571(2)
α (°)	102.748(5)	113.8490(10)	68.600(10)
β (°)	105.557(5)	91.9000(10)	89.300(10)
γ (°)	96.144(5)	106.6370(10)	69.570(10)
V (Å^3)	1303.8(10)	1256.43(17)	1271.1(3)
Z	2	1	1
D_{calc} (g cm^{-3})	1.62	1.557	1.423
μ (Mo) (mm^{-1})	2.185	2.629	1.132
λ (MoKα) (Å)	0.71069	0.71073	0.71073
F(000)	632	596	560
T (K)	295(2)	110(2)	295(2)
Reflections collected	5076	14352	4590
Reflections observed [$I > 2\sigma(I)$]	4392	5127	2526
Parameters	310	298	298
R	0.0292	0.0249	0.0666
R_w (all data)	0.0980	0.0616	0.2290
Goodness-of-fit (GOF) on F^2	1.136	1.051	0.998
	5	**7**	**9**
Empirical formula	$C_{52}H_{52}Br_2Cu_2N_6O_2P_2S_2$	$C_{24}H_{22}CuIN_6O_2S_2$	$C_{52}H_{50}Cl_2Cu_2N_{14}O_4S_4$
Crystal system	triclinic	monoclinic	triclinic
Space group	$P\bar{1}$	$P2_1/c$	$P\bar{1}$
a (Å)	10.9430(9)	16.657	11.2973(5)
b (Å)	11.1806(9)	9.282	11.9516(5)
c (Å)	12.6450(10)	19.705	12.4961(4)
α (°)	112.156(8)	90	93.951(3)
β (°)	90.369(7)	108.37	108.277(3)
γ (°)	109.116(8)	90	112.057(4)
V (Å^3)	1338.86(19)	2891.4	1451.07(10)
Z	1	4	1
D_{calc} (g cm^{-3})	1.496	1.565	1.443
μ (Mo) (mm^{-1})	2.469	1.999	1.025

Table 3 (*continued*)

	1	2	3
λ (MoKα) (Å)	0.71073	0.71073	0.71073
F(000)	612	1352	648
T (K)	200(2)	123(2)	200(2)
Reflections collected	14770	22196	22532
Reflections observed [$I > 2\sigma(I)$]	8342	9598	9582
Parameters	308	325	352
R	0.0377	0.0413	0.0320
R_w (all data)	0.1027	0.0930	0.0769
Goodness-of-fit (GOF) on F^2	1.010	0.921	0.891

Table 4
Important bond parameters (bond lengths (Å) and bond angles (°)).

$[Cu_2(\mu\text{-}I)_2(\eta^1\text{-}S\text{-}HftscMe)_2(Ph_3P)_2]$ **1**			
Cu(1)–S(1)	2.3336(13)	P(1)–Cu(1)–S(1)	118.35(4)
Cu(1)–P(1)	2.2642(12)	P(1)–Cu(1)–I(1)	112.24(3)
Cu(1)–I(1)	2.7010(12)	S(1)–Cu(1)–I(1)	96.11(3)
Cu(1)–I(1)$^{\#1}$	2.7341(9)	P(1)–Cu(1)–I(1)	106.10(3)
S(1)–C(24)	1.693(3)	I(1)–Cu(1)–I(1)$^{\#1}$	108.20(2)
N(1)–N(2)	1.377(4)	Cu(1)–I(1)–Cu(1)	71.80(2)
N(2)–C(24)	1.339(5)	C(24)–S(1)–Cu(1)	110.58(12)
$[Cu_2(\mu\text{-}Br)_2(\eta^1\text{-}S\text{-}HftscMe)_2(Ph_3P)_2]$ **2**			
Cu(1)–S(1)	2.2933(6)	P(1)–Cu(1)–S(1)	112.50(2)
Cu(1)–P(1)	2.2344(6)	P(1)–Cu(1)–Br(1)	112.487(19)
Cu(1)–Br(1)	2.4904(4)	S(1)–Cu(1)–Br(1)	116.590(18)
Cu(1)–Br(1)$^{\#1}$	2.6179(4)	P(1)–Cu(1)–Br(1)	107.429(19)
S(1)–C(6)	1.704(2)	Br(1)–Cu(1)–Br(1)$^{\#1}$	97.397(11)
N(1)–N(2)	1.376(2)	Cu(1)–Br(1)–Cu(1)	82.603(11)
N(2)–C(6)	1.353(3)	C(6)–S(1)–Cu(1)	112.84(8)
$[Cu_2(\mu\text{-}Cl)_2(\eta^1\text{-}S\text{-}HftscMe)_2(Ph_3P)_2]$ **3**			
P(1)–Cu	2.226(2)	P(1)–Cu–S(1)	113.16(9)
S(1)–Cu	2.292(2)	P(1)–Cu–Cl	117.14(8)
Cl–Cu	2.353(2)	S(1)–Cu–Cl	115.66(8)
Cl–Cu	2.573(2)	P1 –Cu –Cl	104.53(8)
C(19)–N(2)	1.336(10)	Cl–Cu–Cl	93.44(7)
N(2)–N(3)	1.383(8)	Cu–Cl–Cu	86.56(7)
C(19)–S(1)	1.692(8)	C(19)–S(1)–Cu	112.7(3)
$[Cu_2(\mu\text{-}Br)_2(\eta^1\text{-}S\text{-}HftscEt)_2(Ph_3P)_2]$ **5**			
Cu–S	2.2866(8)	P–Cu–S	109.71(3)
Cu–P	2.2361(7)	P–Cu–Br	117.03(2)
Cu–Br	2.4887(5)	S–Cu–Br	116.68(2)
Cu–Br$^{\#1}$	2.6005(5)	P–Cu–Br	107.60(2)
S–C(6)	1.697(2)	Br–Cu–Br$^{\#1}$	96.827(14)
N(1)–N(2)	1.375(3)	Cu–Br–Cu	83.173(14)
N(2)–C(6)	1.334(3)	C(6)–S–Cu	113.97(9)
$[CuI(\eta^1\text{-}S\text{-}HftscPh)_2]$ **7**			
I–Cu	2.5479(4)	S(1B)–Cu–S(1A)	109.88(3)
Cu–S(1B)	2.2367(7)	S(1B)–Cu–I	123.83(2)
Cu–S(1A)	2.2422(8)	S(1A)–Cu–I	126.27(2)
S(1A)–C(6A)	1.706(3)	C(6A)–S(1A)–Cu	109.64(10)
S(1B)–C(6B)	1.706(3)	C(6B)–S(1B)–Cu	109.80(9)
$[Cu_2Cl_2(\mu\text{-}S\text{-}HftscPh)_2(\eta^1\text{-}S\text{-}HftscPh)_2]$ **9**			
Cu–S(1A)	2.2617(4)	S(1A)–Cu–S(1B)	108.223(16)
Cu–S(1B)	2.2829(5)	S(1A)–Cu–Cl	120.942(16)
Cu–Cl	2.3306(4)	S(1B)–Cu–Cl	120.547(15)
Cu–S(1B)$^{\#1}$	2.7583(5)	S(1A)–Cu–S(1B)$^{\#1}$	103.356(15)
S(1A)–C(6A)	1.6843(15)	S(1B)–Cu–S(1B)$^{\#1}$	99.546(15)
N(1A)–N(2A)	1.3757(17)	Cl–Cu–S(1B)$^{\#1}$	99.483(14)
N(2A)–C(6A)	1.3436(18)	C(6A)–S(1A)–Cu	110.72(5)

$^{\#1}$ –x, –y, –z.

vary in the order, **1** (2.3336(13)) > **2** (2.2933(6)) > **3** (2.292(3)) Å due to the electronegativity differences of halogen atoms.

Keeping the halogen constant, for example, in complexes of copper(I) bromide, Cu–S bond distance decreases when methyl substituent at N^1 (**2**: 2.2933(6) Å) is replaced by the bulkier ethyl group (**5**: 2.2866(8) Å) and it is attributed to the higher positive inductive effect of ethyl group leading to the strengthening of the Cu–S bond. The Cu–X and Cu–P bond distances in complexes **1**, **3** and **5** are close to the literature value [25,26].

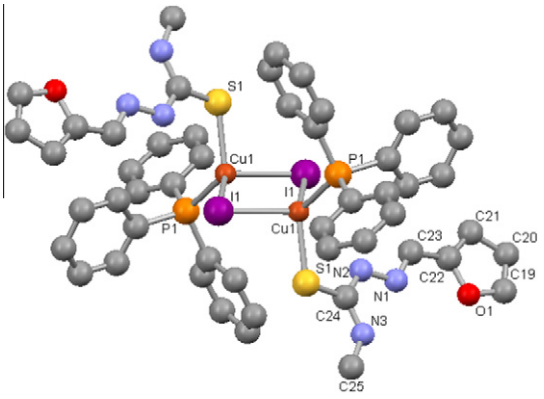

Fig. 1. Structure of iodide bridged dimer $[Cu_2(\mu\text{-}I)_2(\eta^1\text{-}S\text{-}HftscMe)_2(Ph_3P)_2]$ **1** (complexes **2**, **3** and **5** have similar structures).

Bond angles around each copper atom in these complexes lie in the range, 71.80–118.35°, representing distorted tetrahedral geometry in these complexes. In complexes of Hftsc-N^1HMe, the angle Cu–X–Cu at halogen atom of the central core, $Cu(\mu\text{-}X)_2Cu$, increases with the decrease in size of the halogen atom (X = I, 71.80° **1**; Br, 82.603° **2**; Cl, 86.56° **3**) and opposite is the trend for the bond angle X–Cu–X at Cu metal center (X = I, 108.20(2)° **1**; Br, 97.397(11)° **2**; Cl, 93.44(7)° **3**).

Table 1 shows variations in the bond parameters of iodo-bridged dinuclear complexes. The Cu–S distances show variation by changing the substituents at C^2 carbon. In case of the iodo-bridged dimers, the Cu–S distance is less with the aliphatic substituent at C^2 (Me, H, 2.3017(2); Me, Me, 2.3098(2) Å) of thiosemicarbazone than the aromatic or heterocyclic substituents and is probably due to the +I effect of methyl groups. With R^1, R^2 = Me, H and Me, Me, the angle at copper (I–Cu–I) is much smaller than with R^1 = furan, pyrrole, thiophene or phenyl groups. The Cu···Cu separation varies with R^1, R^2 substituents phenyl = furan < pyrrole < thiophene < dimethyl < methyl. A change of substituent at N^1 atom also influences the bond parameters. For example, in case of thiophene-2-carbaldehyde thiosemicarbazone, the Cu–S distance increases as H is changed by methyl group (2.3284(3) Å, H; 2.3306(4) Å, Me), however, the reverse is true for furanaldehyde thosemicarbazone (2.340(9) Å, H; 2.336(18) Å, Me). The same trend is observed with Cu···Cu separation.

There is one sulfur-bridged dimer, namely, complex, $[Cu_2Cl_2(\mu\text{-}S\text{-}Hftsc\text{-}^1HPh)_2(\eta^1\text{-}S\text{-}Hftsc\text{-}N^1HPh)_2]\cdot 2CH_3CN$ **9**. Here Cu^I is bonded to one Cl, and two S donor atoms in species, $CuCl(Hftsc\text{-}N^1HPh)_2$, which has dimerised via thione sulfur (Fig. 2). One bridging Cu–S distance in $Cu(\mu\text{-}S)_2Cu$ core is much longer 2.7583(5) Å than the other (2.2829(5) Å). The former distance is more than the sum of ionic radii of Cu^+ and S^{2-}, 2.61 Å [34]. Unlike the methyl or ethyl substituents, the phenyl group has prevented PPh_3 coordination. It appears that the negative inductive effect of phenyl at N^1 atom lowers Lewis basicity of S donor atom and copper(I) bonded to

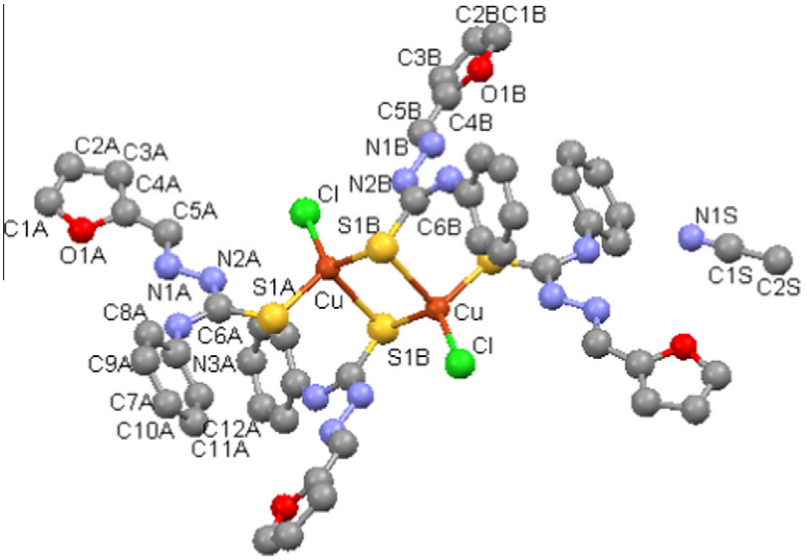

Fig. 2. Structure of sulfur-bridged dimer $[Cu_2Cl_2(\mu\text{-S-Hftsc-N}^1\text{HPh})_2(\eta^1\text{-S-Hftsc-N}^1\text{HPh})_2]\cdot 2CH_3CN$ **9**.

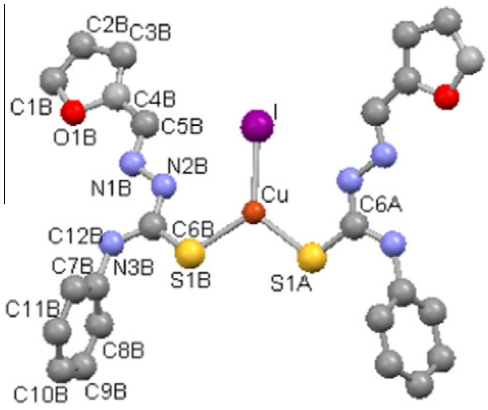

Fig. 3. Structure of $[CuI(\eta^1\text{-S-HftscPh})_2]$ **7**.

Only complex **7** is three coordinate**.** Here Cu is bonded to two S atoms of two thio-ligands and one iodide. The Cu–S bond lengths are 2.2367(7), 2.2422(8) Å. The bond angles around copper ranges, 109.88–126.27°, indicates distorted planar geometry. Comparison of some important bond parameters of three-coordinated monomers is given in Table 2. The three coordinate complexes have been formed: (i) with copper(I) iodide for Ph, Ph (R^1, R^2) at C^2 carbon [35], (ii) with copper(I) halides for thiophene and hydrogen (R^1, R^2) at C^2 along with phenyl (R^3) at N^1 atom [25], (iii) with copper(I) chloride for phenyl and hydrogen (R^1, R^2) at C^2 along with methyl (R^3) at N1 atom [36] and with copper(I) iodide for furan and hydrogen (R^1, R^2) at C^2 along with phenyl (R^3) at N^1 atom [This work]. The Cu–S bond distance increases in order: R^1, R^2: benzophenone < furan < thiophene (iodide halogen). The X–Cu–S angles vary in close range, 119–124, while S–Cu–S angles have range, 109–122°.

more electronegative Cl then prefers to pick up two S atoms of thio-ligands with subsequent dimerization. The bond angles around each copper atom lie in range, 108.22–120.94°. A comparison of important bond parameters of sulfur-bridged dimers with formula, $[Cu_2X_2(\mu\text{-S-Htsc})_2(\eta^1\text{-S-Htsc})_2]$ is given in Table 1. Keeping R^1, R^2 and halogen constant (R^1, C_5H_5O; R^2, H; X = Cl), angle at sulfur has been markedly changed when methyl group (R^3) at N^1 is replaced by phenyl group (Me, 69.89(11)°, Ph, 80.454(5)°). This increase in angle at sulfur also increases the Cu···Cu separation (Me, 2.8060(3) Å; Ph, 3.276 Å). The steric hindrance by bulkier phenyl group may be the reason for this change.

3.3. Packing of complexes (H-bonding networks)

The intermolecular H-bonding is an interesting feature of these complexes. In complex **1**, one of the methyl hydrogen at N^1 atom is intermolecularly connected with the furan ring, namely $H_2\text{-}CH\cdots\pi_{furan}$ (2.772 Å) interaction. Additionally, the $CH_{furan}\cdots\pi_{ph}$ (2.855, 2.803 Å) H-bonding leads to the formation of H-bonded 1D polymer (Fig. 4). However, the more electronegative bromine atom in **2** has changed the H-bonding pattern. The bromine-hydrogen ($Br\cdots HC_{Ph}$, 2.838 Å) H-bonding generated a 1D polymer along the a-axis, which is further engaged in $CH_{Ph}\cdots\pi$, 2.537 Å H-bond-

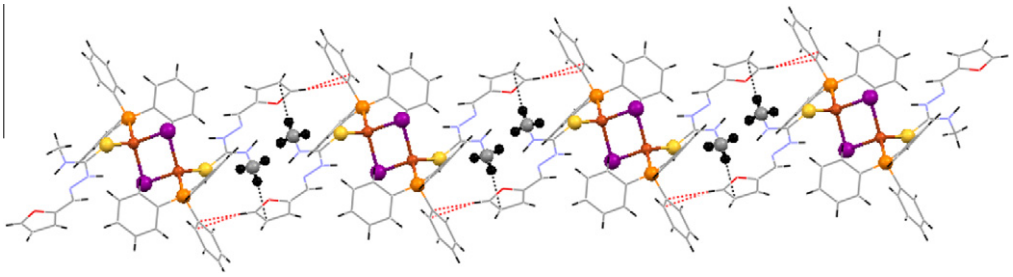

Fig. 4. Packing network of $[Cu_2(\mu\text{-I})_2(\eta^1\text{-S-HftscMe})_2(Ph_3P)_2]$ **1**.

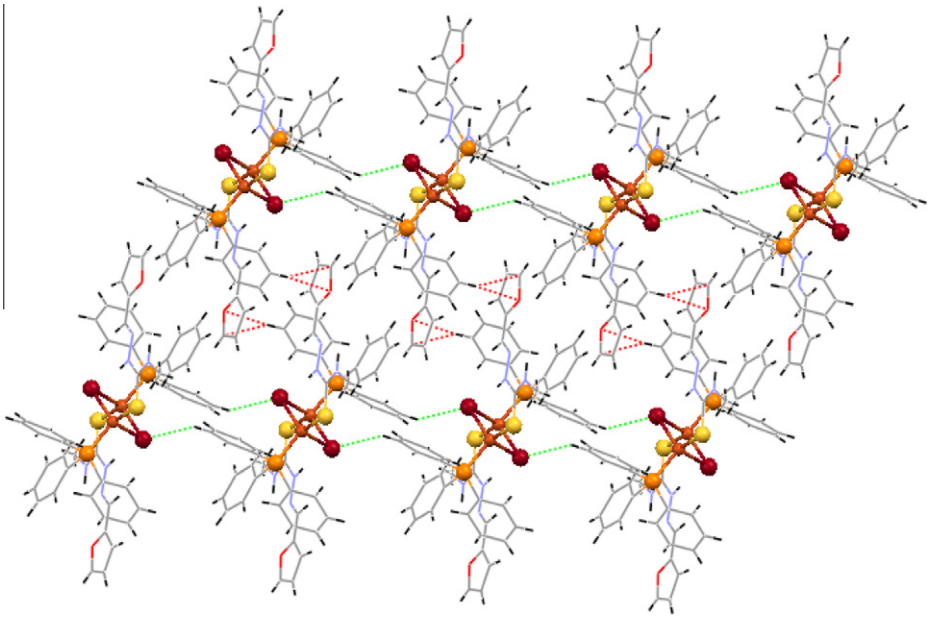

Fig. 5. Packing network of dinuclear complex, $[Cu_2(\mu\text{-}Br)_2(\eta^1\text{-}S\text{-}HftscMe)_2(Ph_3P)_2]$ **2**.

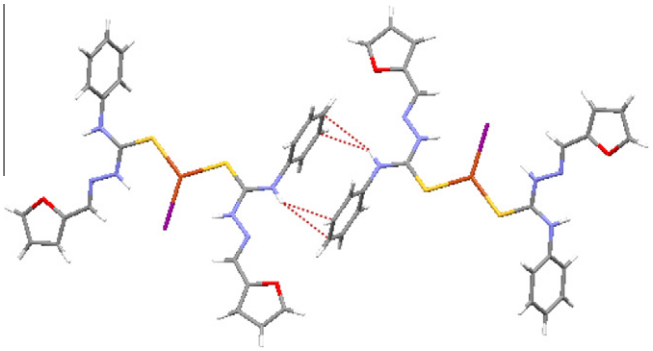

Fig. 6. Packing network of three coordinate complex, $[CuI(\eta^1\text{-}S\text{-}HftscPh)_2]$ **7**.

ing along b axis to form a 2D polymer (Fig. 5). Complexes **3** and **5** exhibited similar type of H-bonding.

In complex **7**, there is only intermolecular, {$PhN^1H\cdots\pi(Ph)$, 2.721, 2.824 Å} interaction present, which results in the formation of dimer (Fig. 6). No other interaction is found in this complex. In complex **9**, the phenyl substituent at N^1 interacts intermolecularly with the chlorine atom via $CH_{(Ph)}\cdots Cl$, 2.879 Å to yield a 1D polymer (Fig. 7). Two layers of acetonitrile molecules are present above and below the 1D layer and are held in position by H-bonding between amino hydrogen and nitrogen of acetonitrile .i.e. $PhN^1H\cdots N$, 2.249 Å interaction.

3.4. Solution phase studies

The ^1H NMR spectra reveal downfield shift in N^2H signals in complexes **1**–**9** vis-à-vis the free ligands (HftscMe, δ 10.80 ppm; HftscEt, δ 10.84 ppm; HftscPh, 11.36 ppm) and it reveals coordination of neutral ligands to the copper metal center in each complex. Further, the C^2H signals of free ligands (HftscMe, δ 7.86 ppm; HftscEt, δ 7.87 ppm; HttscPh, δ 9.29 ppm) undergo downfield shifts in complexes **1**–**6** {δ 8.17–8.89 ppm} and upfield shift in **7**–**9** (δ 8.78–8.98 ppm). The ring protons of Ph_3P, which appeared in the range, δ 7.29–7.53 ppm, have obscured N^1HR^2 proton signals in these complexes. The methyl protons of $-N^1HCH_3$ appear as a doublet in the range, δ 3.19–3.20 ppm in complexes **1**–**3**. The ethyl pro-

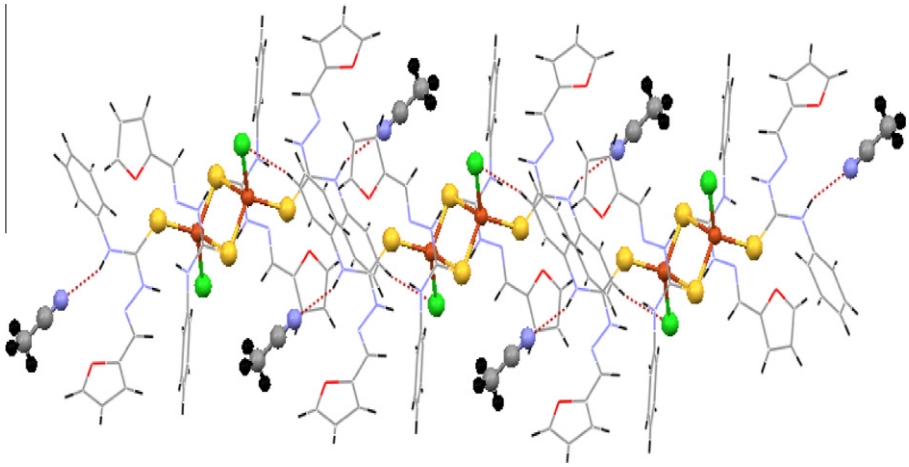

Fig. 7. Packing network of $[Cu_2Cl_2(\mu\text{-}S\text{-}HftscPh)_2(\eta^1\text{-}S\text{-}HftscPh)_2]\cdot 2CH_3CN$ **9**.

tons of $-N^1HC_2H_5$ group appear as two sets, one multiplet (δ 3.63–3.69 ppm, CH_2); and one triplet (δ 1.31–1.33 ppm, CH_3) in complexes **4**–**6**. The phenyl protons of $-N^1HC_6H_5$ appear in the range, δ 7.24–7.60 ppm in **7**–**9**, which also incorporate $-N^1H$ protons. It is pointed out here that the solution phase studies appear to be in line with the solid state studies.

4. Conclusion

Furan-2-carbaldehyde thiosemicarbazones $\{(C_4H_3O)HC^2{=}N^3{-}N(H){-}C^1(=S)N^1HR\}$ with methyl/ethyl (HftscMe/HftscEt) substituents at N^1 nitrogen have favored halogen-bridged dinuclear complexes with copper(I) halides (X = Cl, Br, I), namely, $[Cu_2(\mu\text{-}X)_2(\eta^1\text{-}S\text{-}L)_2(PPh_3)_2]$, a behavior similar to that of N^1-substituted thiophene-2-carbaldehyde thiosemicarbazones. The presence of phenyl at N^1 has yielded a three-coordinated complex with copper(I) iodide and sulfur-bridged dimers with copper(I) chloride/bromide, namely, $[Cu_2X_2(\eta^1\text{-}S\text{-}HL)_2(\mu\text{-}S\text{-}HL)_2]$, where no PPh_3 was coordinating and this is unlike that shown by thiophene-2-carbaldehyde-N^1-phenyl-thiosemicarbazone [25].

Acknowledgements

Financial assistance from CSIR (Scheme No.: 01(1993)/05/EMR-II), New Delhi is gratefully acknowledged.

Appendix A. Supplementary data

CCDC 860067–860072; contains the supplementary crystallographic data for **1**–**3**, **5**, **7** and **9**. These data can be obtained free of charge via http://www.ccdc.cam.ac.uk/conts/retrieving.html, or from the Cambridge Crystallographic Data Centre, 12 Union Road, Cambridge CB2 1EZ, UK; fax: (+44) 1223 336 033; or e-mail: deposit@ccdc.cam.ac.uk. Supplementary data associated with this article can be found, in the online version, at http://dx.doi.org/10.1016/j.poly.2012.08.014.

References

[1] T.S. Lobana, Rekha Sharma, Gangandeep Bawa, Sonia Khanna, Coord. Chem. Rev. 253 (2009) 977.
[2] S.B. Padhye, G. Kauffman, Coord. Chem. Rev. 63 (1985) 127.
[3] D.X. West, S.B. Padhye, P.B. Sonawane, Struct. Bonding (Berlin Ger.) 76 (1991) 4.
[4] D.X. West, A.E. Liberta, S.B. Padhye, R.C. Chikate, P.B. Sonawane, A.S. Kumbhar, R.G. Yerande, Coord. Chem. Rev. 123 (1993) 49.
[5] J.S. Casas, M.S. Garcia-Tasende, J. Sordo, Coord. Chem. Rev. 209 (2000) 197.
[6] D.R. Smith, Coord. Chem. Rev. 164 (1997) 575.
[7] T.S. Lobana, S. Khanna, R. Sharma, G. Hundal, R. Sultana, M. Chaudhary, R.J. Butcher, A. Castineiras, Cryst. Growth Design 8 (2008) 1203.
[8] R.K. Mahajan, I. Kaur, T.S. Lobana, Talanta 59 (2003) 101.
[9] R.K. Mahajan, I. Kaur, T.S. Lobana, Ind. J. Chem. 45A (2006) 639.
[10] R.K. Mahajan, T.P.S. Walia, Sumanjit, T.S. Lobana, Talanta 67 (2005) 755.
[11] L.S. Sarma, J.R. Kumar, C.J. Kumar, A.V. Reddy, Anal. Lett. 36 (2003) 605.
[12] K.J. Reddy, J.R. Kumar, C. Ramachandraiah, T. Thriveni, A.V. Reddy, Food. Chem. 101 (2007) 585.
[13] M.A. Ali, M.E. Khalifa, S.E. Ghazy, M.M. Hassanien, Anal. Sci. 18 (2002) 1235.
[14] U. Abram, K. Ortner, R. Gust, K. Sommer, J. Chem. Soc. Dalton Trans. (2000) 735.
[15] K. Nomiya, K. Sekino, M. Ishiawa, A. Honda, M. Yokoyama, N.C. Kasuga, H. Yokoyama, S. Nakano, K. Onodera, J. Inorg. Biochem. 98 (2004) 601.
[16] M.B. Ferrari, F. Bisceglie, G. Pelosi, P. Tarasconi, R. Albertini, A. Bonati, P. Lunghi, S. Pinelli, J. Inorg. Biochem. 83 (2001) 169.
[17] D.X. West, J.S. Ives, J. Krejci, M.M. Salberg, T.L. Zumbahlen, G.A. Bain, A.E. Liberta, J. Valdes-Martinez, S. Hernadez-Ortiz, R.A. Toscano, Polyhedron 14 (1995) 2189.
[18] J. Garcia-Tojal, L. Lezama, J.L. Pizarro, M. Insausti, M.I. Arriortua, T. Rojo, Polyhedron 18 (1999) 3703.
[19] E.M. Jouad, G. Larcher, M. Allain, A. Riou, G.M. Bouet, M.A. Khan, X.D. Thanh, J. Inorg. Biochem. 86 (2001) 565.
[20] V.G. Puranik, S.S. Tavale, T.N.G. Row, P. Umapathy, A.P. Budhkar, Acta Crystallogr., Sect. C: Cryst. Struct. Commun. 43 (1987) 2303.
[21] T.S. Lobana, R.J. Rekha, A. Butcher, E. Castineiras, P.V. Bermejo, Bharatam, Inorg. Chem. 45 (2006) 1535.
[22] R.J. Butcher, D.X. West, Transition Met. Chem. 18 (1993) 449.
[23] E.M. Jouad, A. Riou, M. Allain, M.A. Khan, G.M. Bouet, Polyhedron 20 (2001) 67.
[24] Y. Kang, N. Yang, S.-O. Kang, J. Ko, C.-H. Lee, Y.-H. Lee, Organometallics 16 (1997) 5522.
[25] T.S. Lobana, R. Sharma, A. Castineiras, G. Hundal, R.J. Butcher, Inorg. Chim. Acta 362 (2009) 3547.
[26] T.S. Lobana, Rekha Sharma, Z. Anorg, Allg. Chem. 635 (2009) 2150.
[27] G. Brauer, Handbook of Preparative Chemistry, vol. 2, second ed., Academic Press, New York, 1965.
[28] XSCANS, Siemens Analytical X-ray Instruments Inc., Madison, WI, USA, 1994.
[29] International Tables for X-ray Crystallography, vol. C, Kluwer, Dordrecht, The Netherlands, 1995.
[30] Bruker. SMART and SAINT. Area Detector Control and Integration Software, Bruker Analytical X-ray Instruments Inc., Madison, Wisconsin, USA, 1997.
[31] G.M. Sheldrick, SADABS. Program for empirical absorption correction of area detector data, University of Goettingen, Germany, 1997.
[32] G.M. Sheldrick, Acta Cryst. A46 (1990) 467.
[33] G.M. Sheldrick, SHELXL-97. Program for the refinement of crystal structures, University of Goettingen, Germany, 1997.
[34] J.E. Huheey, E.A. Keiter, R.L. Keiter, Inorganic chemistry: Principles of structure and reactivity, 4th edit, Harper Collins College, New York, 1993.
[35] T.S. Lobana, S. Khanna, R.J. Butcher, A.D. Hunter, Polyhedron 25 (2006) 2755.
[36] T.S. Lobana, P. Kumari, A. Castineiras, R.J. Butcher, J. Coord. Chem. 62 (2009) 1754.
[37] T.S. Lobana, S. Khanna, R.J. Butcher, Z. Anorg, Allg. Chem. 633 (2007) 1820.
[38] T.S. Lobana, S. Khanna, G. Hundal, R.J. Butcher, A. Castineiras, Polyhedron 28 (2009) 3899.
[39] T.S. Lobana, Rekha, R.J. Butcher, Transition Met. Chem. 29 (2004) 291.